Development and initial commissioning of the FAUST-QTS experimental beam line

P. Cammarata, A. B. McIntosh, M. B. Chapman, G. A. Souliotis, L. Bakthiari, S. Behling, G. Bonasera, L. A. Heilborn, K. Hagel, Z. Kohley, J. Mabiala, L. W. May, A. Raphelt, M. D. Youngs, A. Zarrella, and S. J. Yennello

The nuclear Equation-of-State (EoS) describes the thermodynamic properties from nuclei to neutron stars spanning a wide range of densities, temperatures and neutron-proton asymmetries [1–5]. Thus, the understanding of the EoS is important to understanding not only the reaction dynamics of heavy-ion collisions but also for describing astrophysical processes such as the formation of neutron stars and the dynamical collapse of supernovae [6–9] in addition to nuclear physics problems including understanding the structure of rare, exotic nuclei[10, 11]. Constraining the density dependence of the asymmetry energy (E_{sym}) [12–15], which describes how the EoS depends on the nucleon asymmetry of nuclear matter, $\frac{N-Z}{N+Z}$,can be probed via a number of sensitive observables. Many of these observables can been seen from heavy-ion collisions [13, 16–24], neutron skin thicknesses measurements [10, 25–28], and astrophysical measurements [1–5, 15, 29–31]. The observables from heavy-ion collisions change not only as a function of beam energy but also as a function of impact parameter, time evolution of the reacting system and the resulting products.

The scope of the initial commissioning phase of this campaign is focused on examining the dynamical break-up of the projectile- and target-like fragments from heavy-ion collisions. Specifically, we are interested in investigating the reaction mechanism competition involved to produce heavy ($Z\geq3$) 3- or 4-body breaking of the reacting system at low-intermediate energy (~15 MeV/nucleon). In this specific case, it has been proposed that the isospin content, alignment and velocity distributions of the excited primary fragments, shape deformations of the heaviest fragments, and observables (multiplicity, isospin content, angular alignment, etc) associated with the emission of fragments from the low-density neck region produced in mid-peripheral heavy ion collisions represent observables sensitive to the EoS [20, 32–37]. This particular experiment attempts to measure a significant fraction of the observables from both the heavy, projectile-like fragments (PLFs) near the beam axis as well as the emitted intermediate mass fragments (IMFs) and light charged particles (LCPs) at lower intermediate energies, together, for a more complete picture of a majority of the charged particles in the event. In particular we are interested in measuring the heavy residues both near the beam axis in a Quadrupole Triplet Spectrometer (QTS), as well as in the Forward Array Using Silicon Technology[42] (FAUST). This is combined with measuring lighter particles (IMFs and LCPs) in the FAUST array that should provide for better characterization of the event. Data collected for the purposes of this experiment were from reactions of 15 MeV/nucleon ^{136}Xe,^{124}Sn+^{64}Ni and ^{124}Xe+^{58}Ni using the K500 Super-conducting cyclotron at Texas A&M University. Table I tabulates the reaction systems and their isospin asymmetry.

Table I. System to system isospin asymmetry

System	$\delta = \frac{N-Z}{A}$
^{136}Xe + ^{64}Ni	0.1800
^{124}Sn + ^{64}Ni	0.1702
^{124}Xe + ^{58}Ni	0.0989

The FAUST array has been coupled to the QTS which was previously used for RIB/facility upgrade experiments with BIGSOL[41, 43–46]. The new arrangement (Figs. 1 and 2) combines the FAUST array and the QTS for Time- of-Flight (ToF) mass measurements of heavy fragments in FAUST and the QTS for heavy PLFs/EVRs as well as ΔE-E measurements for isotopic resolution of LCPs/Light IMFs (Z≤10) and Z identification of heavier IMFs (up to the beam in some cases). The ToF mass identification in FAUST is achieved via newly designed integrated charge sensitive,

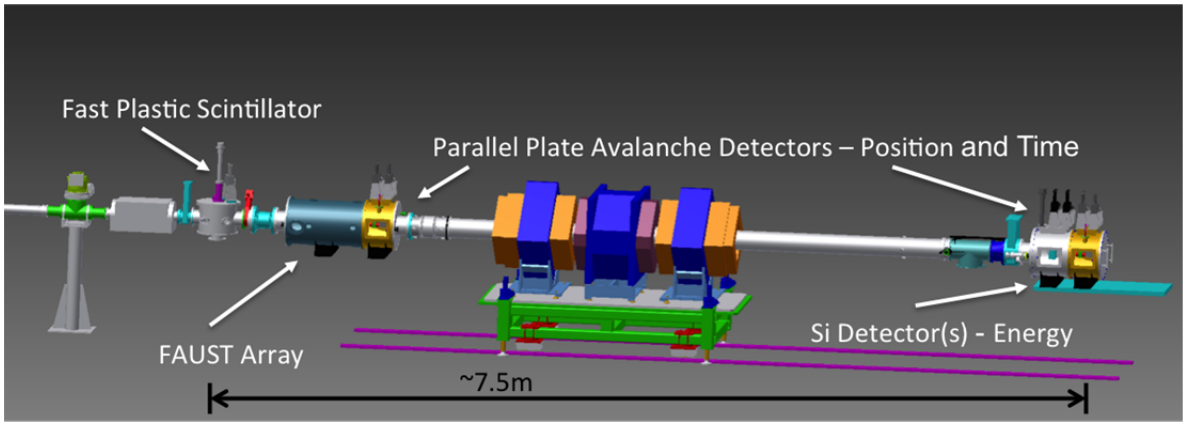

FIG. 1. Rendered CAD schematic of the FAUST-QTS beam line. The projectile is transported from the left to the right. The projectile generates a timing signal in the Fast Plastic used for both timing in FAUST and measuring beam intensity. After reacting with the target, IMFs, LCPs and PLFs are measured by a range of techniques in FAUST. The QTS has been coupled to FAUST to measure, through a narrow angular and $\beta\rho$ acceptance, the time-of-flight and energy of PLFs that escape through the throat of FAUST. This is accomplished through timing between the PPACs and energy resolved by the silicon detectors at the end of the spectrometer.

timing pickoff (CS/TPO) preamplifier upgrade to FAUST combined with a thin film, fast plastic time-zero detector up-stream of FAUST. The ToF mass measurements in the QTS were made using Parallel Plate Avalache Counters (PPACs)[47] for accurate time of flight coupled with a Si semiconductor detector at θ=0◦ at the back of the FAUST-QTS line. In forward focused intermediate energy nuclear reactions, this arrangement allows for large efficiency collection of the resultant PLF as well as emitted LCPs and IMFs.

FIG. 2. Actual picture of the FAUST-QTS line assembled and vacuum tight ready to be populated with detectors and cabled to data acquisition electronics. Picture taken in April 2013.

I. SIMULATIONS

Both Deep Inelastic Transport (DIT) [48] and Constrained Molecular Dynamics [49] models were use to generate PLFs in the range of interest. The results from DIT were statistically cooled by GEMINI [50] where as the CoMD was allowed to dynamically cool out to t=3000fm/c. The results of both were then analyzed through RAYTRACE [51] to approximate the efficiency and the resulting distributions at the Si detector after the QTS. Additionally, COSY-Infinity [52] was utilized to take into account possible 3rd order (or greater) effects, final approximation of magnetic current settings required, and visualization of the $\beta\rho$ dependent flight pattern through the QTS.

Simulations using COSY-Inifinity were examined to explore the effects of higher order aberrations on the lab-frame coordinate distribution of the particles of interest at the QTS Si detector. Higher order effects on the focusing of the particles of interest were observed to be dramatic for small changes (±5%) in $\beta\rho$. Based on these simulations we found that defocusing the last magnet in the QTS by 10%, allowed for a lower degree of aberration at the focal point. This effect was expected due to the asymmetric flight path length in the current configuration. Final current and magnetic field settings were determined empirically while tuning the primary beam on phosphorescent viewers and initial transport of particles of interest through the PPACs which allowed us to look at the lab-frame distribution of reaction

products in real time. The predictions by COSY-Infinity were consistent within error of the electrical current fluctuations of the magnet power supplies. The resultant flight path of a representative PLF emitted at $\theta = 1^{\circ}$ and $\beta\rho = 1.48$Tm through FAUST-QTS is shown in Fig. 3 as the red line. We can see for small changes of ±5% in $\beta\rho$, represented by the other differently colored lines, that significant efforts in particle focusing and collimation are required to reliably transport only the particles of interest to the focal plane. This, combined with coincidence measurements in FAUST and small angular and $\beta\rho$ acceptance of the QTS, provides for the ability to more efficiently filter and trigger on PLFs of interest while decreasing the number of scattered beam particles.

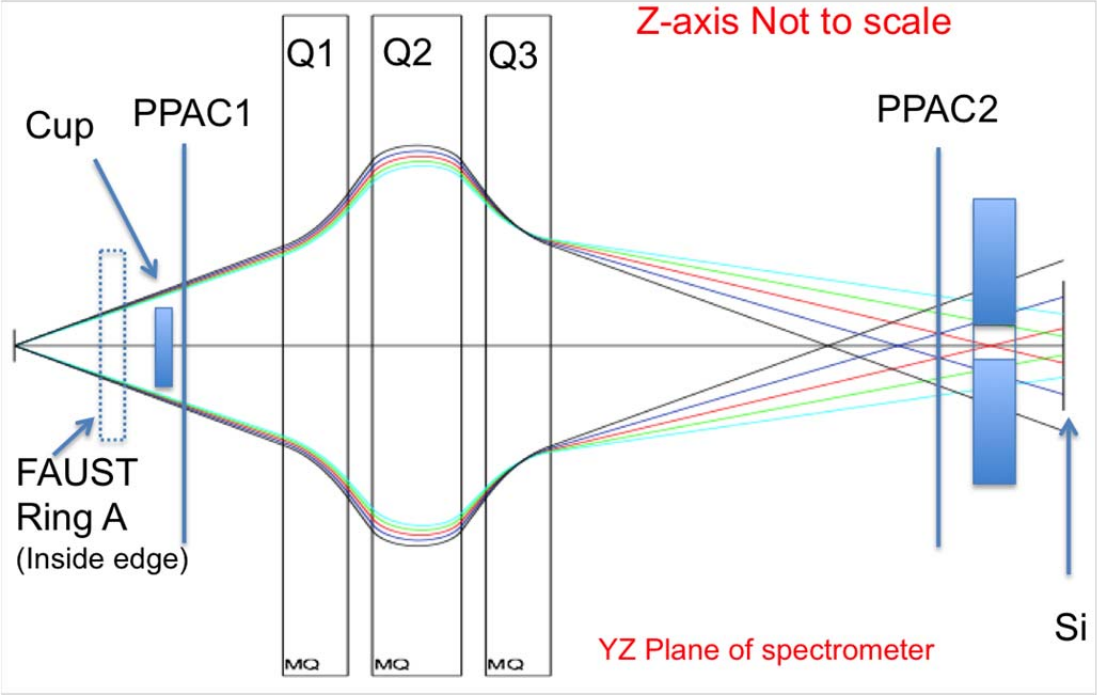

FIG. 3. Visualization of COSY-Inifity transport of the PLF emitted at $\theta = 1^{\circ}$ and $\beta\rho = 1.48$Tm through FAUST-QTS. Each color represents a shift of ± 5% increments in $\beta\rho$ where the red line is the PLF of interest (0%), +5%(black), +10% (blue), -5% (green) and -10% (light blue) deviation in $\beta\rho$. Efficient use of collimation and detector positioning, in conjunction with dynamics simulation fed transport approximations, allow for experimental filtering and triggering more effeciently on PLFs of interest while decreasing the number of scattered beam particles. Since the $\beta\rho$ of the PLF is near to that of the beam-like projectile scatter, attenuation of the beam-like scattered particles is accomplished through collimation and accurate de-focusing in combination with coincidence discrimination as provided by emitted particles detected in FAUST.

II. EXPERIMENTAL RESULTS

In keeping with the stated physics goal of the commissioning experiment, we have detected and reconstructed the hot, quasi-projectile like fragments resulting from a ternary breakup of the reaction system. Specifically, the breakup of the reaction system into three particles with Z≥3 is of interest to the community with respect to observing mechanism competition and the possible influence of the asymmetry energy in lower intermediate energy heavy-ion collisions. In this scenario, the projectile and target interacting and separating into a hot quasi-projectile and quasi- target. Because of detector thresholds and geometry, we are only able to detect the ternary breakup of the reaction system where the quasi-projectile (QP) breaks into a PLF and IMF. We then approximate the composition and energy of the quasi-target via momentum and mass conservation by assuming that all other particles are contained or are emitted from the quasi-target. This event selection requires that we are able to identify an IMF in FAUST in coincidence with another particle of Z≥3 in either FAUST or the QTS. The event-by-event multiplicity = 2 for particles of Z≥3 represents a small number of, not only, events with a particles of Z≥3, as seen in Fig. 4, but also represents less than 1% of the total number of events detected. Beam-like

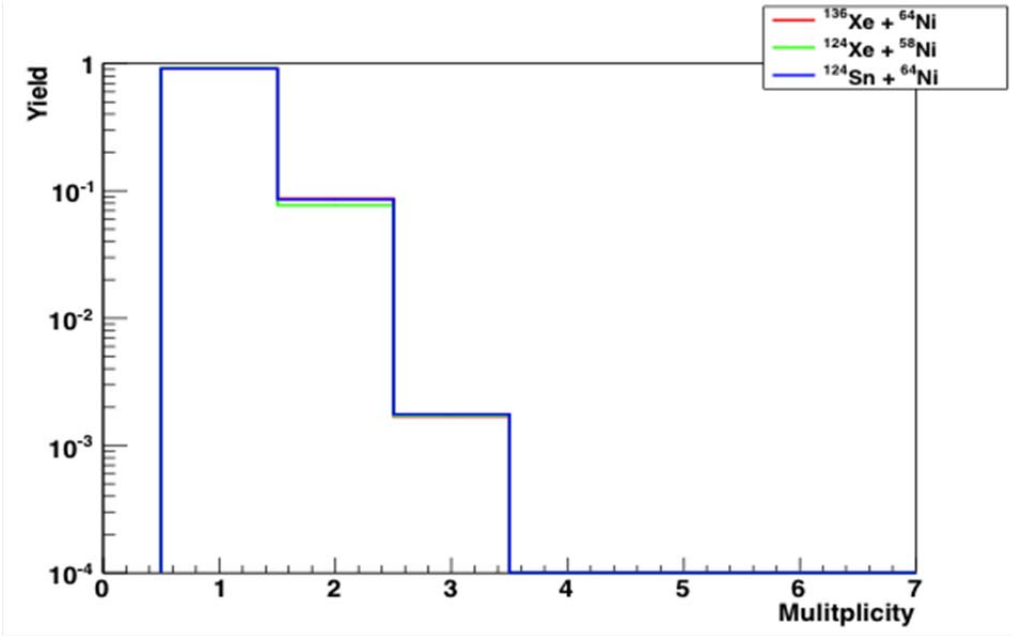

FIG. 4. Event multiplicity for particles with Z≥3. Events of interest are multiplicity = 2 because of FAUST-QTS is not able to detect target like particles. Because of this the target like particles are approximated by momentum and mass conservation and thus not explicity included in this multiplicity distribution.

particles identified in coincidence with the initial FAUST identified particle are removed from the data. Additionally, the reconstructed QP must have an energy E_{QP} >25%·E_{beam} . For the events that pass this criterion, a large number of these events are forward focused with a majority of the detected PLFs detected in the QTS (low perpendicular velocity in the lab frame) and all of the IMFs detected in FAUST (swath at higher values of perpendicular velocity) as shown in Fig. 5.

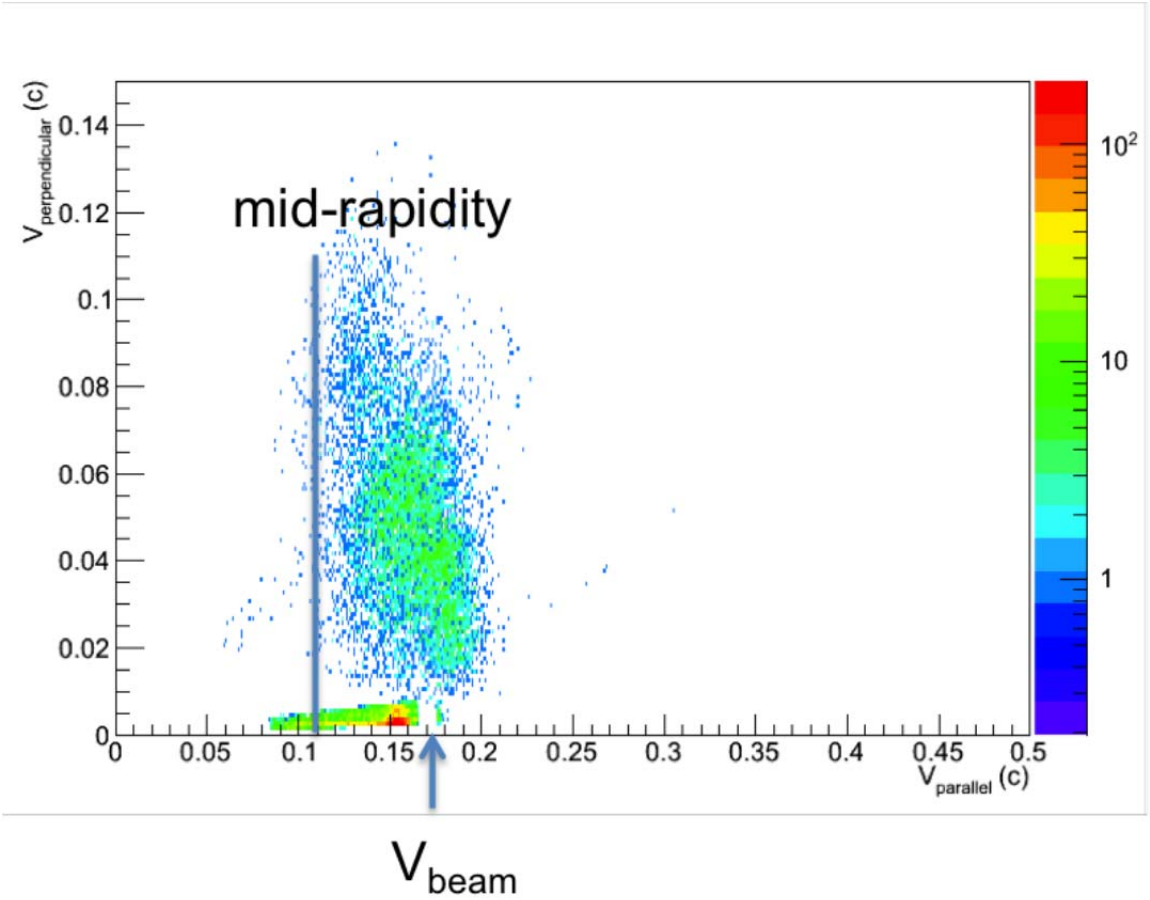

FIG. 5. $V_{perpendicular}$ vs $V_{parallel}$ for events with a multiplicity = 2 for particles with Z≥ meeting the criterion stated in the text.

[1] T. Klähn, D. Blaschke, S. Typel, E.N.E. van Dalen, A. Faessler, C. Fuchs, T. Gaitanos, H. Grigorian, A. Ho, E.E. Kolomeitsev *et al.*, Phys. Rev. C **74**, 035802 (2006).

[2] P. Danielewicz, R. Lacey, and W.G. Lynch, Science **298**, 1592 (2002).

[3] A. Steiner, M. Prakash, J. Lattimer, and P. Ellis, Phys. Rep. **411**, 325 (2005).

[4] A.W. Steiner, J.M. Lattimer, and E.F. Brown, Astrophys. J. **722**, 33 (2010).

[5] J.M. Lattimer and M. Prakash, Science **304**, 536 (2004).

[6] W. Hix, O. Messer, A. Mezzacappa, M. Liebendörfer, J. Sampaio, K. Langanke, D. Dean, and G. Martínez-Pinedo, Phys. Rev. Lett. **91**, 201102 (2003).

[7] C.J. Horowitz and J. Piekarewicz, Phys. Rev. Lett. **86**, 5647 (2001).

[8] S. Gandolfi, J. Phys. Conf. Ser. **420**, 012150 (2013).

[9] A. Bauswein, T.W. Baumgarte, and H.-T. Janka, Phys. Rev. Lett. **111**, 131101 (2013).

[10] B.A. Brown, Phys. Rev. Lett. **85**, 5296 (2000).

[11] R. Furnstahl, Nucl. Phys. **A706**, 85 (2002).

[12] P. Möller, W.D. Myers, H. Sagawa, and S. Yoshida, Phys. Rev. Lett. **108**, 052501 (2012).

[13] M.B. Tsang, J.R. Stone, F. Camera, P. Danielewicz, S. Gandolfi, K. Hebeler, C.J. Horowitz, J. Lee, W.G. Lynch, Z. Kohley *et al.*, Phys. Rev. C **86**, 015803 (2012).
[14] I. Tews, T. Krüger, K. Hebeler, and A. Schwenk, Phys. Rev. Lett. **110**, 032504 (2013).
[15] A.W. Steiner, J.M. Lattimer, and E.F. Brown, Astrophys. J. Lett. **765**, L5 (2013).
[16] M.B. Tsang, T.X. Liu, L. Shi, P. Danielewicz, C.K. Gelbke, X.D. Liu, W.G. Lynch, W.P. Tan, G. Verde, A. Wagner *et al.*, Phys. Rev. Lett. **92**, 062701 (2004).
[17] M.B. Tsang, Y. Zhang, P. Danielewicz, M. Famiano, Z. Li, W.G. Lynch, and A.W. Steiner, Phys. Rev. Lett. **102**, 122701 (2009).
[18] Z. Kohley, M. Colonna, A. Bonasera, L.W. May, S. Wuenschel, M. Di Toro, S. Galanopoulos, K. Hagel, M. Mehlman, W.B. Smith *et al.*, Phys. Rev. C **85**, 064605 (2012).
[19] Z. Kohley, G. Christian, T. Baumann, P.A. DeYoung, J.E. Finck, N. Frank, M. Jones, J.K. Smith, J. Snyder, A. Spyrou *et al.*, Phys. Rev. C **88**, 041601 (2013).
[20] V. Baran, M. Colonna, M. Di Toro, V. Greco, M. Zielinska-Pfabe, and H. Wolter, Nucl. Phys. **A703**, 603 (2002).
[21] E. Geraci, M. Bruno, M. D'Agostino, E. DeFilippo, A. Pagano, G. Vannini, M. Alderighi, A. Anzalone, L. Auditore, V. Baran *et al.*, Nucl. Phys. **A732**, 173 (2004).
[22] M.A. Famiano, T. Liu, W.G. Lynch, M. Mocko, A.M. Rogers, M.B. Tsang, M.S. Wallace, R.J. Charity, S. Komarov, D.G. Sarantites *et al.*, Phys. Rev. Lett. **97**, 052701 (2006).
[23] D. Shetty, S.J. Yennello, A. Botvina, G. Souliotis, M. Jandel, E. Bell, A. Keksis, S. Soisson, B. Stein, and J. Iglio, Phys. Rev. C **70**, 011601 (2004).
[24] G.-C. Yong, B.-A. Li, L.-W. Chen, and W. Zuo, Phys. Rev. C **73**, 034603 (2006).
[25] P.A. Souder, R. Holmes, C.-M. Jen, L. Zana, Z. Ahmed, A. Rakhman, and E. Cisbani *et al.*, PAC38 (2010).
[26] X. Roca-Maza, M. Centelles, X. Vinas, and M. Warda, Phys. Rev. Lett. **106**, 252501 (2011).
[27] S. Ban, C.J. Horowitz, and R. Michaels, J. Phys. G **39**, 015104 (2012).
[28] W. Horiuchi, Y. Suzuki, and T. Inakura, Phys. Rev. C **89**, 011601 (2014).
[29] P.B. Demorest, T. Pennucci, S.M. Ransom, M.S.E. Roberts, and J.W.T. Hessels, Nature **467**, 1081 (2010).
[30] K. Hebeler, J.M. Lattimer, C.J. Pethick, and A. Schwenk, Astrophys. J. **773**, 11 (2013).
[31] M. Prakash, Proc. Sci. 8th Int. Work. Crit. Point Onset Deconfinement (2013).
[32] R. Lionti, V. Baran, M. Colonna, and M. Di Toro, Phys. Lett. B **625**, 33 (2005).
[33] M. Colonna, J. Phys. Conf. Ser. **168**, 012006 (2009).
[34] V. Baran, M. Colonna, and M. Di Toro, Nucl. Phys. **A730**, 329 (2004).
[35] C. Rizzo, V. Baran, M. Colonna, A. Corsi, and M. Di Toro, Phys. Rev. C **83**, 014604 (2011).
[36] M. Di Toro, V. Baran, M. Colonna, G. Ferini, T. Gaitanos, V. Greco, J. Rizzo, and H. Wolter, Nucl. Phys. **A787**, 585 (2007).
[37] L. Shvedov, M. Colonna, and M. Di Toro, Phys. Rev. C **81**, 054605 (2010).
[38] H. Savajols and VAMOS Collaboration, Nucl. Phys. **A654**, 1027 (1999).
[39] J. Pouthas, B. Borderie, and R. Dayras, Nucl. Instrum. Methods Phys. Res. **A357**, 418 (1995).
[40] R.E. Tribble, R. Burch, and C. Gagliardi, Nucl. Instrum. Methods Phys. Res. **A285**, 441 (1989).

[41] G. Souliotis, D. Shetty, A. Keksis, E. Bell, M. Jandel, M. Veselsky, and S.J. Yennello, Phys. Rev. C **73**, 024606 (2006).
[42] F. Gimeno-Nogues, D. Rowland, E. Ramakrishnan, S. Ferro, S. Vasal, R. Gutierrez, R. Olsen, Y.-W. Lui, R. Laforest, H. Johnston *et al.*, Nucl. Instrum. Methods Phys. Res. **A399**, 94 (1997).
[43] G.A. Souliotis, A.S. Botvina, D.V. Shetty, A.L. Keksis, M. Jandel, M. Veselsky, and S.J. Yennello, Phys. Rev. C **75**, 011601 (2007).
[44] G.A. Souliotis, A.L. Keksis, B. Stein, M. Veselsky, M. Jandel, D. Shetty, S. Soisson, S. Wuenschel, and S.J. Yennello, Nucl. Instrum. Methods Phys. Res. **B261**, 1094 (2007).
[45] M. Barbui, S. Pesente, G. Nebbia, D. Fabris, M. Lunardon, S. Moretto, G. Viesti, M. Cinausero, G. Prete, V. Rizzi *et al.*, Nucl. Instrum. Methods Phys. Res. **B265**, 605 (2007).
[46] G.A. Souliotis, B. Stein, M. Veselsky, S. Galanopoulos, A. Keksis, Z. Kohley, D. Shetty, S. Soisson, S. Wuenschel, and S.J. Yennello, Nucl. Instrum. Methods Phys. Res. **B266**, 4692 (2008).
[47] D. Swan, J. Yurkon, and D. Morrissey, Nucl. Instrum. Methods Phys. Res. **A348**, 314 (1994).
[48] L. Tassan-Got and C. Stephan, Nucl. Phys. **A524**, 121 (1991).
[49] M. Papa, G. Giuliani, and A. Bonasera, J. Comput. Phys. **208**, 403 (2005).
[50] R. Charity, ICTP-IAEA Adv. Work. Model Codes (2008).
[51] S. Kowalski and H. Enge, Nucl. Instrum. Methods Phys. Res. **A258**, 407 (1987).
[52] K. Makino and M. Berz, Nucl. Instrum. Methods Phys. Res. **A558**, 346 (2006).